

# Lecture 13 – PET

**This lecture will cover:** *(CH3.13-3.21)*

- Positron Emission Tomography (PET)
  - Introduction of PET
  - Radiotracer used for PET/CT
  - Instrumentation of PET/CT
  - PET imaging
  - Data processing in PET/CT
  - Image characteristics
  - Time-of-flight PET
- Clinical applications of PET

*(Supplementary reading: The Essential Physics of Medical Imaging CH19.3)*

# Introduction

- Emission tomography for functional imaging of the body;
- 100-1000 times higher SNR and significantly better spatial resolution than SPECT;
- Based on positron emission reaction and pair production;
- The fundamental difference between SPECT and PET is the radiotracers.
- PET/CT has largely replaced stand-alone PET

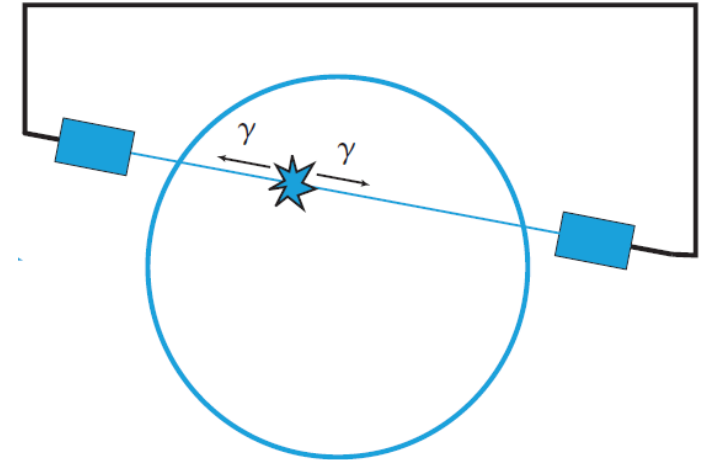


**Fig.** In PET, photon pairs are detected by electronic coincidence circuits connecting pairs of detectors..

# Radiotracer used for PET/CT

- Undergo radioactive decay by emitting a positron



- Isotopes:  $^{11}\text{C}$ ,  $^{15}\text{O}$ ,  $^{18}\text{F}$ ,  $^{13}\text{N}$

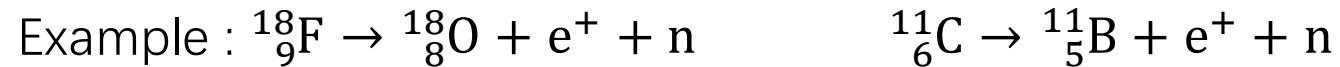


**Table.** Properties and applications of the most common PET radiotracers

Radionuclide	Half-life (minutes)	Radiotracer	Clinical applications
$^{18}\text{F}$	109.7	$^{18}\text{F}$ FDG	oncology, inflammation, cardiac viability
$^{11}\text{C}$	20.4	$^{11}\text{C}$ -palmitate	cardiac metabolism
$^{15}\text{O}$	2.07	$\text{H}_2^{15}\text{O}$	cerebral blood flow
$^{13}\text{N}$	9.96	$^{13}\text{NH}_3$	cardiac blood flow
$^{82}\text{Rb}$	1.27	$^{82}\text{RbCl}_2$	cardiac perfusion

# Radiotracer used for PET/CT

- Radiotracers for PET are structural analogues (类似物) of biologically active molecules in which one or more of atoms have been replaced by a radioactive atom
- Most commonly used Isotopes is  $^{18}\text{F}$ -fluorodeoxyglucose (FDG,  $^{18}\text{F}$  脱氧葡萄糖),

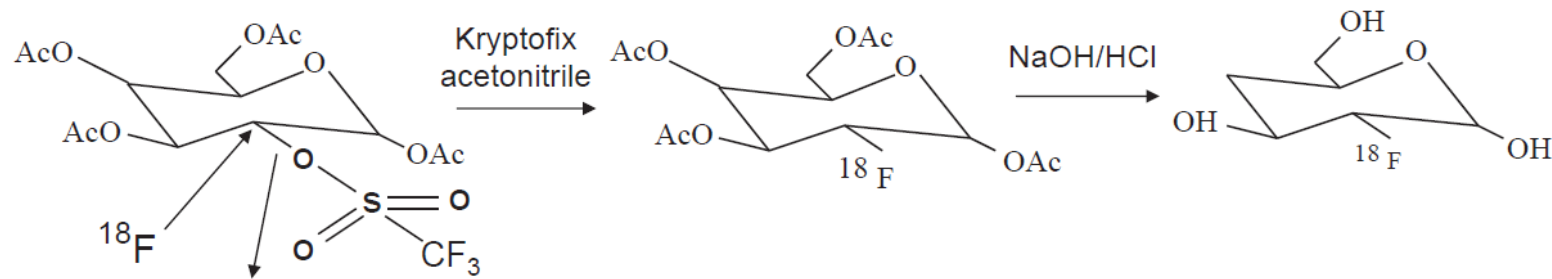


**Figure 3.23**

The most common synthesis of  $^{18}\text{F}$ FDG.

# Radioactive transformation and coincidence

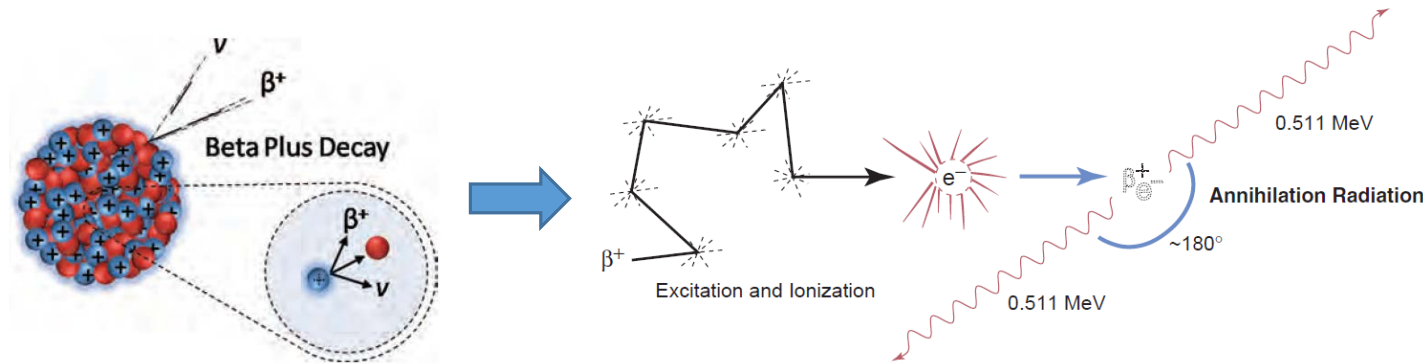
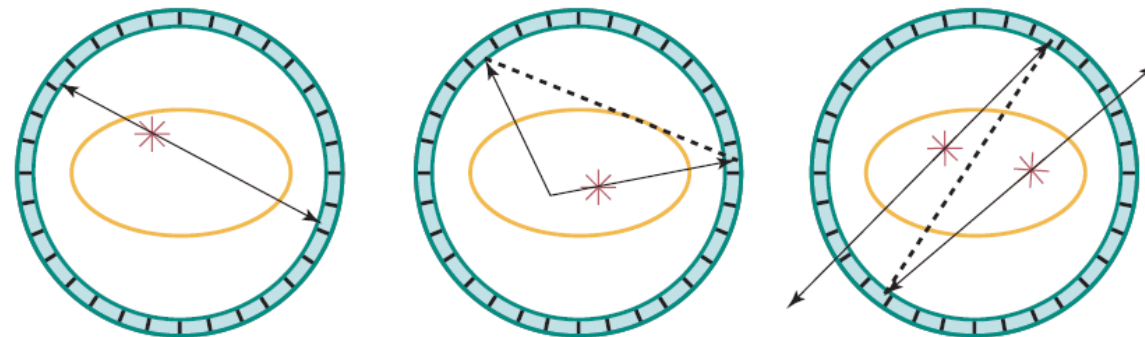


**Fig 1.** (Left) the positron decay; (Right) Annihilation radiation, forms an intrinsic LOR (line-of-reconstruction, or line-of-response).

**Fig 2.** True coincidence (left), scatter coincidence (center), and random (accidental) coincidence (right). A scatter coincidence is a true coincidence, because it is caused by a single nuclear transformation, but results in a count attributed to the wrong LOR (dashed line). The random coincidence is also attributed to the wrong LOR.



# Instrumentations of PET

**Higher SNR and spatial resolution comparing to SPECT due to:**

- Collimation not being required;
- Reduced attenuation of higher energy  $\gamma$ -rays in tissue;
- The use of a complete ring of detector.

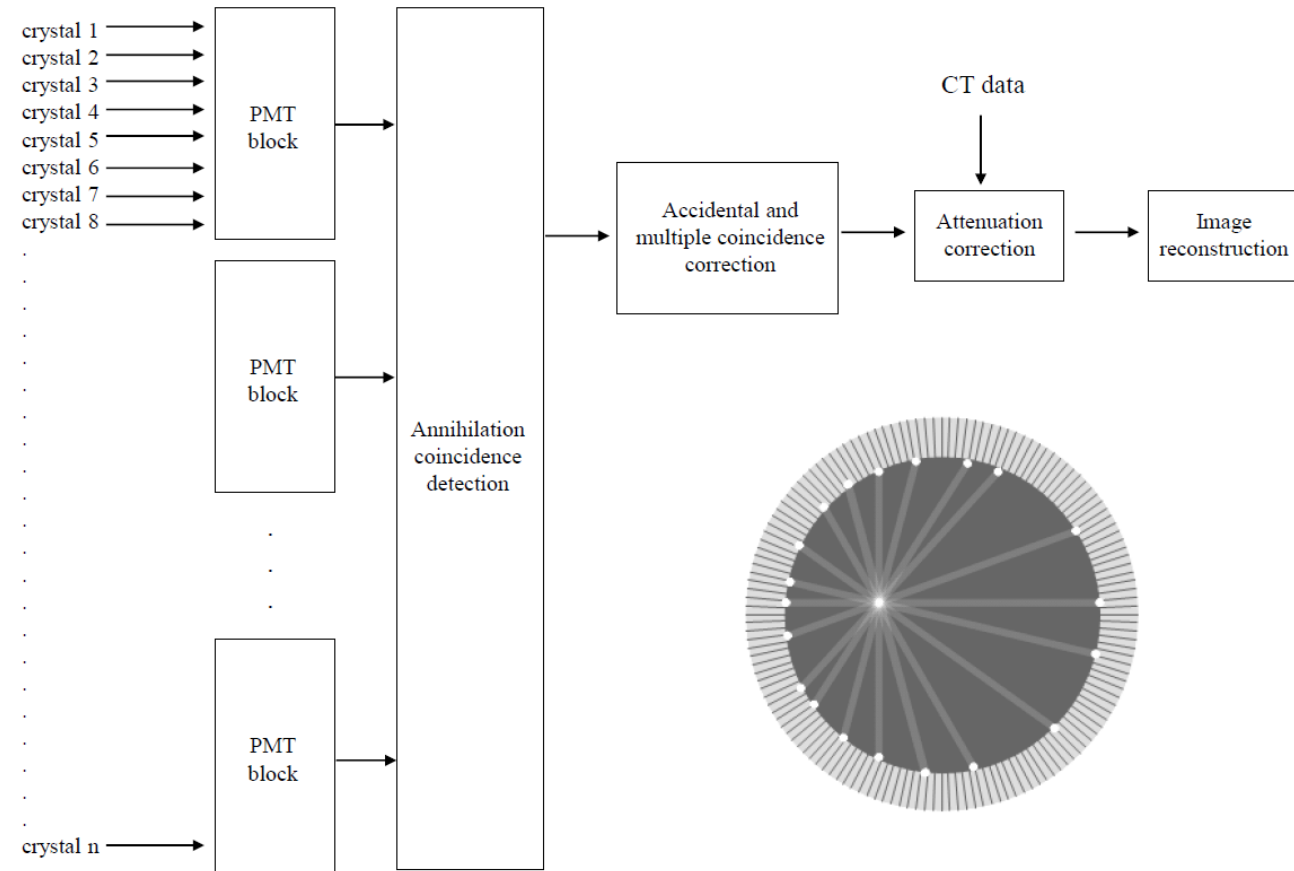


**Fig.** (top) The elements of a PET/CT system. (inset) Formation of lines-of-response in the PET detector ring.

# Detectors for PET

## The ideal detector crystal has:

- A high  $\gamma$ -ray detection efficiency ;
- A short decay time to allow a short coincidence resolving time;
- A high emission intensity to allow more crystals to be coupled to a single PMT;
- An emission wavelength near 400nm for maximum sensitivity for PMTs;
- Optical transparency at the emission wavelength;
- An index of refraction close to 1.5 to ensure efficient transmission of light between crystal and the PMT.

# Properties of PET detectors

	Decay time (ns)	Emission intensity	Efficiency ( $\epsilon^2$ )	$\lambda_{\text{emitted}}$ (nm)	$\eta$
BGO	300	0.15	0.72	480	2.15
LSO(Ce)	40	0.75	0.69	420	1.82
BaF <sub>2</sub>	0.8 <sub>prim</sub> , 600 <sub>sec</sub>	0.12	0.34	220, 310	1.49
GSO(Ce)	60 <sub>prim</sub> , 600 <sub>sec</sub>	0.3	0.57	430	1.85
NaI(Tl)	230 <sub>prim</sub> , 10 <sup>4</sup> <sub>sec</sub>	1.0	0.24	410	1.85

*GSO(Ce): cerium-doped gadolinium orthosilicate ( $\text{Gd}_2\text{SiO}_5$ ), LSO(Ce): cerium-doped lutetium orthosilicate ( $\text{Lu}_2\text{SiO}_5$ ). Both primary and secondary decay times are reported, efficiency values are for 2 cm thickness crystals and represent detection of both  $\gamma$ -rays striking the two detectors,  $\eta$  is the refractive index, and decay times are expressed as primary and secondary decays; the intensity is relative to a value of 1.0 for NaI(Tl).*



# Block detector

- A large block of BGO (dimension of 50\*50\*30mm) with a series of partial cuts through it on the top;
- The cuts is filled with light-reflecting material to prevent light from producing a very broad LSF when reach the bottom of crystal;
- Considered as separate detector array due to the partial cut.
- PMTs couple to Block and localize  $\gamma$ -ray using the same Anger principle as gamma camera.

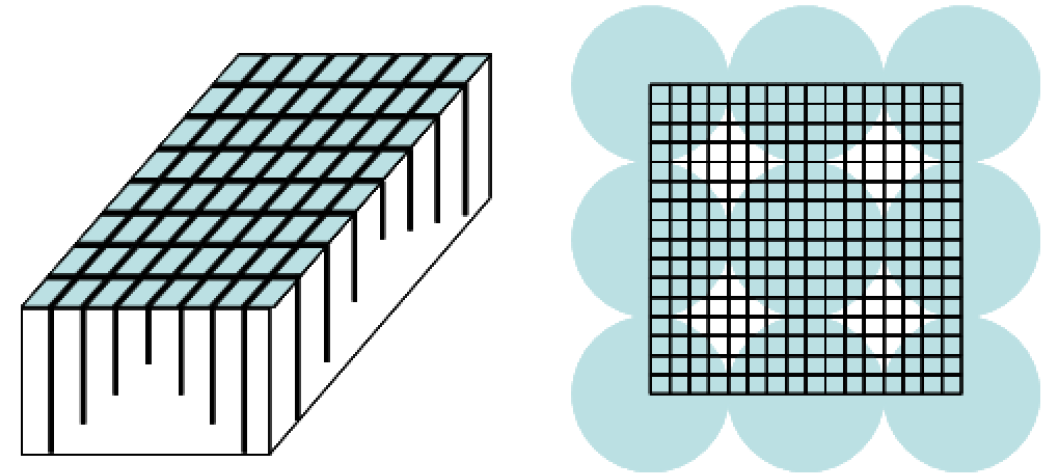


**Fig.** (left) A large BGO crystal cut into 64 effective separate elements. The partial cuts are filled with light-reflecting material. (right) Quadrant-sharing arrangement of the BGO crystals with PMTs shown by the circles..

# PMT and PHA

- The operation of photomultiplier (PMT) and pulse height analyzer (PHA) is identical to the planar scintigraphy and SPECT.
- The voltage within pre-determined range generates a “logic pulse”, typically 6-10ns long
- The pulse is sent to the coincidence detector
- The energy resolution of BGO crystals is  $\sim 20\%$ , therefore the energy window is 450-650keV

# Annihilation coincidence detection

- Coincidence resolving time:
  - the time window that is allowed for a second  $\gamma$ -ray to be recorded and assigned to the same annihilation after the first  $\gamma$ -ray has been detected;
  - Typically value of 6-12ns
- In-coincidence detectors;
- True coincidence: two  $\gamma$ -rays strike the in-coincidence detectors in the coincidence resolving time.
- LOR (line of response, 响应线) can be established between the two detectors with striking  $\gamma$ -rays.

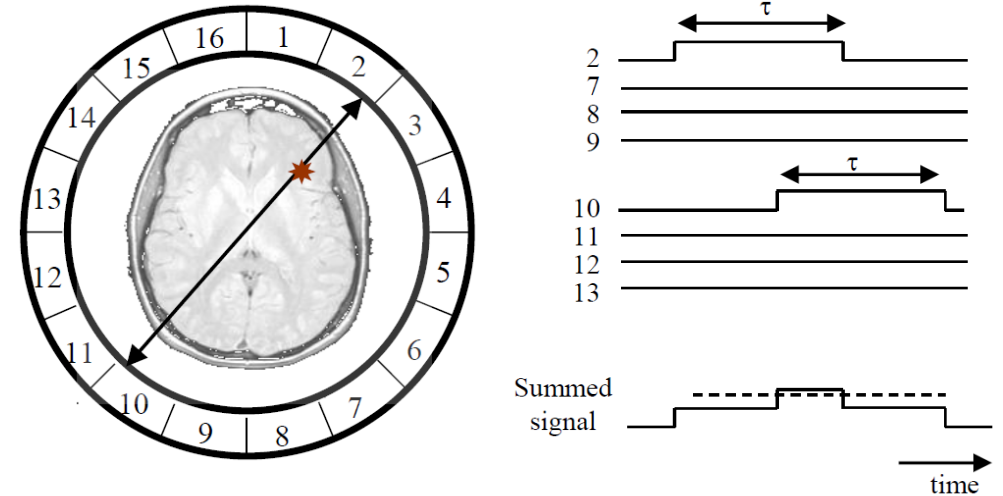


**Fig.** The principle of annihilation coincidence detection. (left) The two  $\gamma$ -rays reach detectors 2 and 10, triggering respective logic pulses of length  $\tau$ . (right) If both logic pulses are sent to the coincidence detector within the system coincidence resolving time  $2\tau$ , then the summed signal lies above the threshold value (dashed line) and a coincidence is recorded.

# 2D & 3D PET Imaging

➤ Retractable lead collimation septa positioned between each rings

- 2D mode: extended septa
- 3D mode: retracted septa

➤ 2D mode

- Reduce the amount of scattered  $\gamma$ -rays detected;
- Produce uniform sensitivity profile along the axial dimension;

- $2n-1$  image planes: image plane can be formed between 2 crystals in the same ring (direct plane) or adjacent rings (cross planes)

➤ 3D mode

- Higher sensitivity by about factor of 10
- Higher SNR and reduced scan time
- More random and scattered coincidence
- Sensitivity is higher in the center than two ends

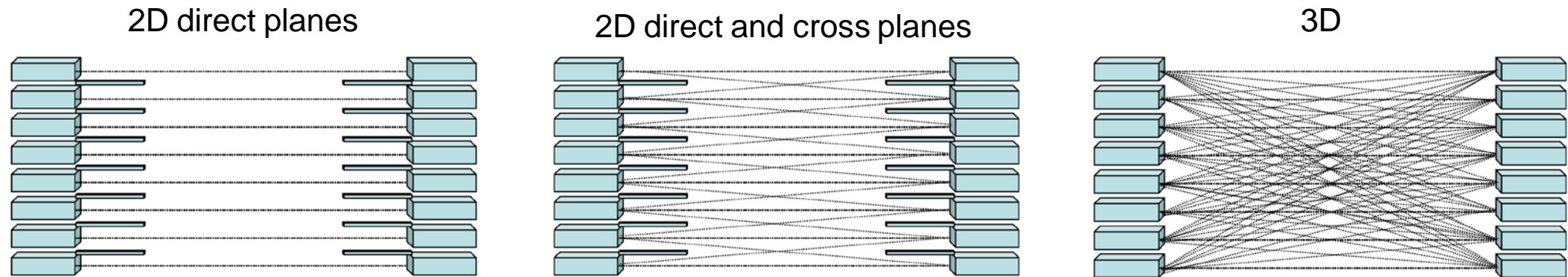


**Fig.** Three different data acquisition modes used for PET scans. Note that the septal collimators are retracted for 3D mode

# Data processing in PET/CT

## ➤ **Attenuation correction**

- Using PET/CT scanner for estimation of attenuation coefficients and anatomical structures.
- Standard attenuation coefficient value assigned at 511keV

## ➤ **Correction for accidental and multiple coincidence**

## ➤ **Correction for scattered coincidence**

## ➤ **Correction for dead time:** The three major sources of dead time in PET

- The time taken to integrate the charge for the PMTs
- The processing of a coincidence event
- The presence of multiple coincidences in which the data are discarded

# Correction for accidental and multiple coincidence

- Accidental (random) coincidence
  - ~20% for head scan and 50% for body scan;
  - Uniformly distribution across imaging FOV
- Methods of correction
  - Additional parallel timing circuitry
    - ✓ The second coincidence timing window starts significantly later (typically 60ns) after an event is recorded
    - ✓ The accidental coincidences are subtracted
  - Uniformly distribution across imaging FOV
    - ✓ The rate of recorded accidental coincidence :  $C_{ij}^{acc} = 2\tau R_i R_j$ , where  $R_i$  and  $R_j$  are the single count rates in the individual detectors  $i$  and  $j$ , and  $2\tau$  is the coincidence resolving time;
    - ✓ Multiple coincidence:  $M_{ij} \approx C_{ij}^{acc} \tau R_{ij} N_{ij}$ , where  $N_{ij}$  is the total number of detectors operating in coincidence with either of the two detector  $i$  and  $j$ .

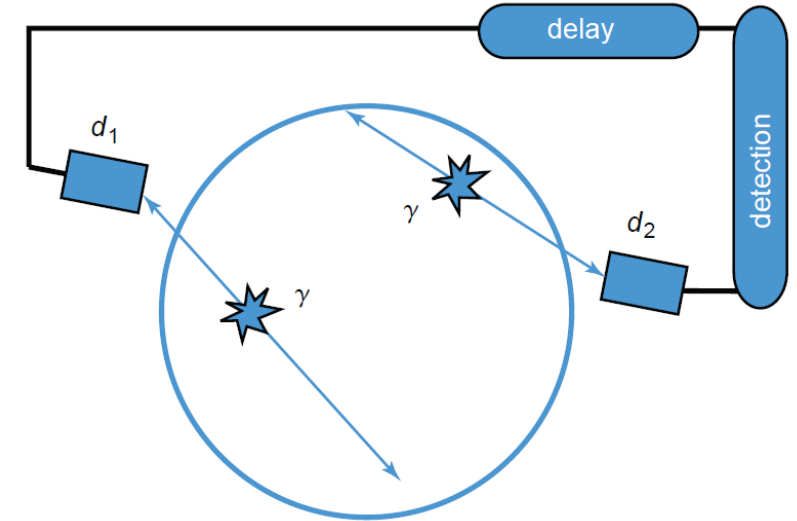


**Fig.** Schematic representation of a random and its detection. One of the two photons is detected with a small time delay...

# Correction for scattered coincidence

- Major sources of scattered radiation for PET signals
  - Scatter within the body.
  - Scatter in the BGO crystal due to poor intrinsic energy resolution
- ~10-15% for 2D PET, and up to 50% for 3D PET
- Correction methods
  - Measure the signal intensity in areas that are outside patient and fit to a Gaussian shape to estimate scatter inside the patient
  - Multiple energy window method
  - Iterative reconstruction based on simulating the actual scatter using CT-derived attenuation maps

# Image characteristics

## ➤ **Signal-to-noise ratio**

- **Similar influence factors as SPECT:** radiotracer dose, targeting efficiency, imaging acquisition time,  $\gamma$ -rays attenuation in the patient, system sensitivity, image post-processing, etc
- **Higher SNR than SPECT due to higher sensitivity:** in the same condition of  $\gamma$ -ray radioactivity, 0.01-0.03% for SPECT, 0.2-0.5% for PET 2D mode, 2-10% for PET 3D mode.

## ➤ **Contrast-to-noise:** in addition to SNR, influenced by

- The correction for in Compton-scattered  $\gamma$ -rays
- The non-specific uptake of radiotracer in healthy tissue surrounding the pathology being studied.



# Image characteristics

## ➤ Spatial resolution

- The in-plane resolution is much more constant throughout the patient: the inherent “double detection” of two  $\gamma$ -rays reduce the depth dependence of the PSF
- Other factors affecting resolution
  - ✓ The effective positron range in tissue before it annihilates with an electron: 0.2-2.6mm for different radiotracer;
  - ✓ The non-collinearity of the two  $\gamma$ -rays, i.e. the small random deviation from  $180^\circ$ : with FWHM of approximately  $0.5^\circ$
  - ✓ The dimensions of the detector crystals: an approximate spatial resolution given by half the detector diameter.
- Overall resolution of the system:  $R_{\text{sys}} \approx \sqrt{R_{\text{detector}}^2 + R_{\text{range}}^2 + R_{180^\circ}^2}$
- Typical FWHM of system resolution: 3-4mm for a small ring system for brain studies, 5-6mm for a larger whole-body system

# PET/CT

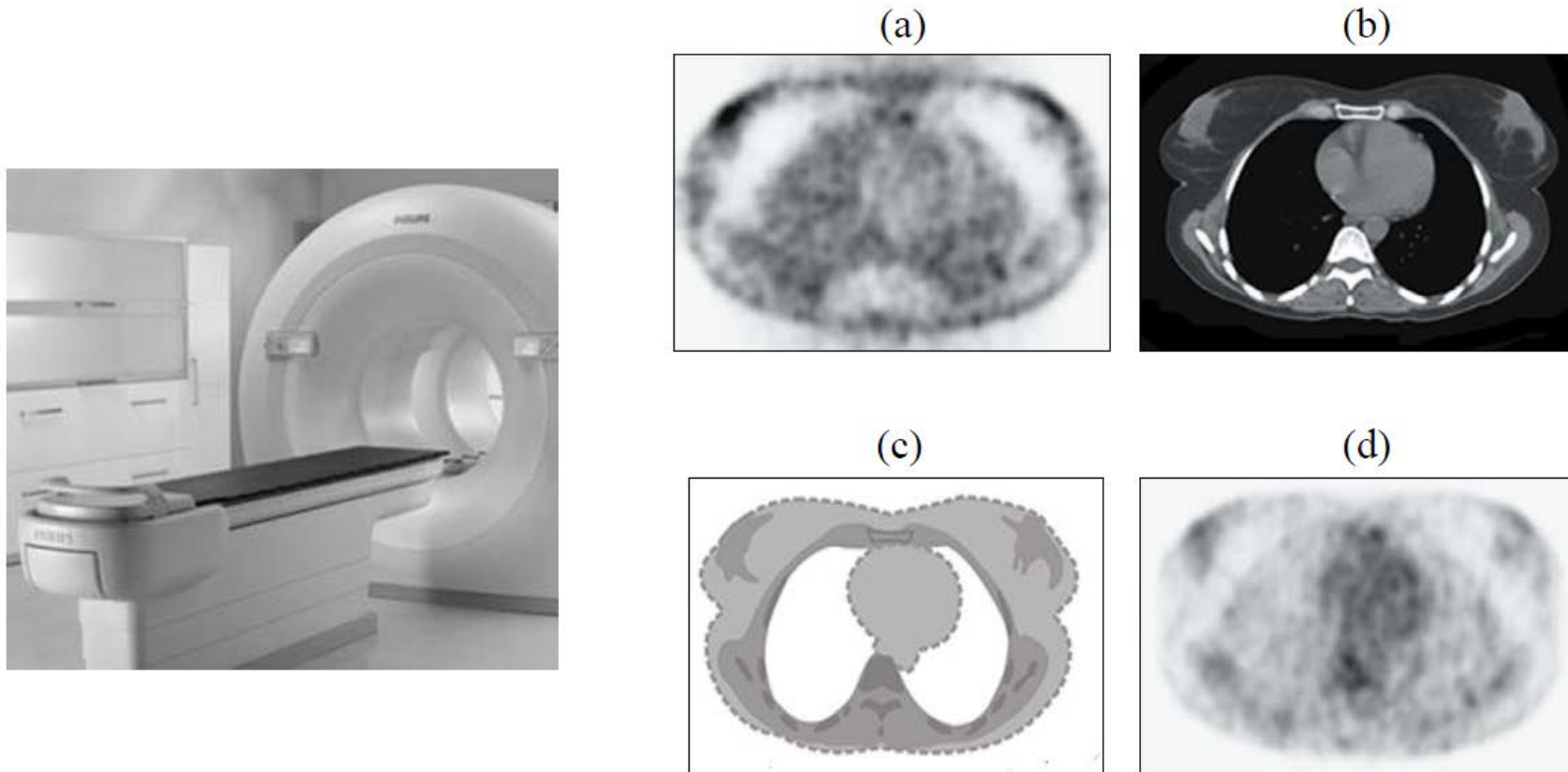


**Fig.** (left) A PET/CT scanner with two separate rings of detectors. A common bed slides the patient through the two scanners. (right) (a) An uncorrected PET, (b) a CT image, (c) the CT-derived attenuation map after segmentation of the CT image, and (d) the attenuation-corrected PET scan.

# Time-of-flight PET

## Time-of-flight (TOF, 飞行时间) PET

- Estimating position on the constrained LOR defined by the time difference corresponding to the delay between the two  $\gamma$ -rays;
- The position resolution:  $\Delta x = c\Delta t/2$ , where  $\Delta t$  is the timing resolution,  $c$  is the speed of light
- Constrained LOR reduces the statistical noise since the noise variance is proportional to the length of LOR.
- The multiplicative reduction factor of noise:

$$f = \frac{D}{\Delta x} = \frac{2D}{c\Delta t}$$

where  $D$  is the size of patient

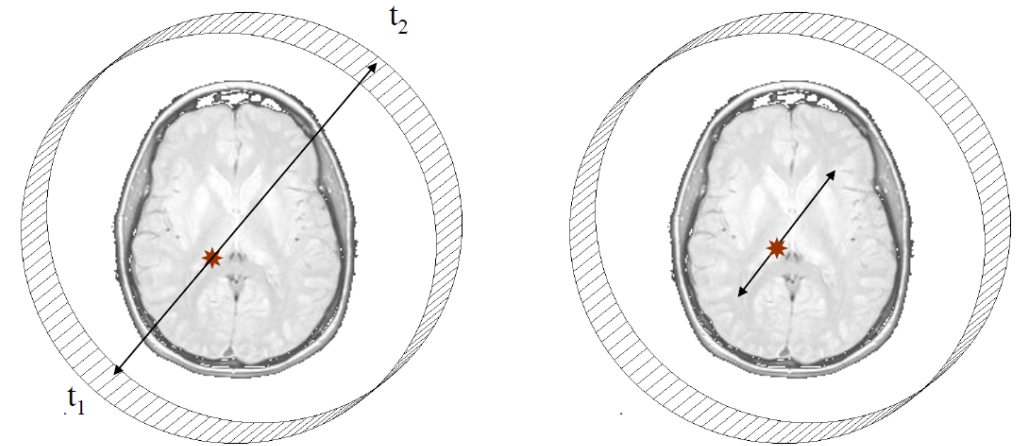


**Fig.** (left) Conventional LOR formed in PET. (right) Constrained LOR in TOF-PET defined by the time difference  $t_2 - t_1$  corresponding to the delay between the two  $\gamma$ -rays striking the particular detectors..

# **Lecture 13 – PET**

## **This lecture will cover:**

- Positron Emission Tomography (PET)
  - Introduction of PET
  - Radiotracer used for PET/CT
  - Instrumentation of PET/CT
  - PET imaging
  - Data processing in PET/CT
  - Image characteristics
  - Time-of-flight PET
- **Clinical applications of PET**

# Tumors

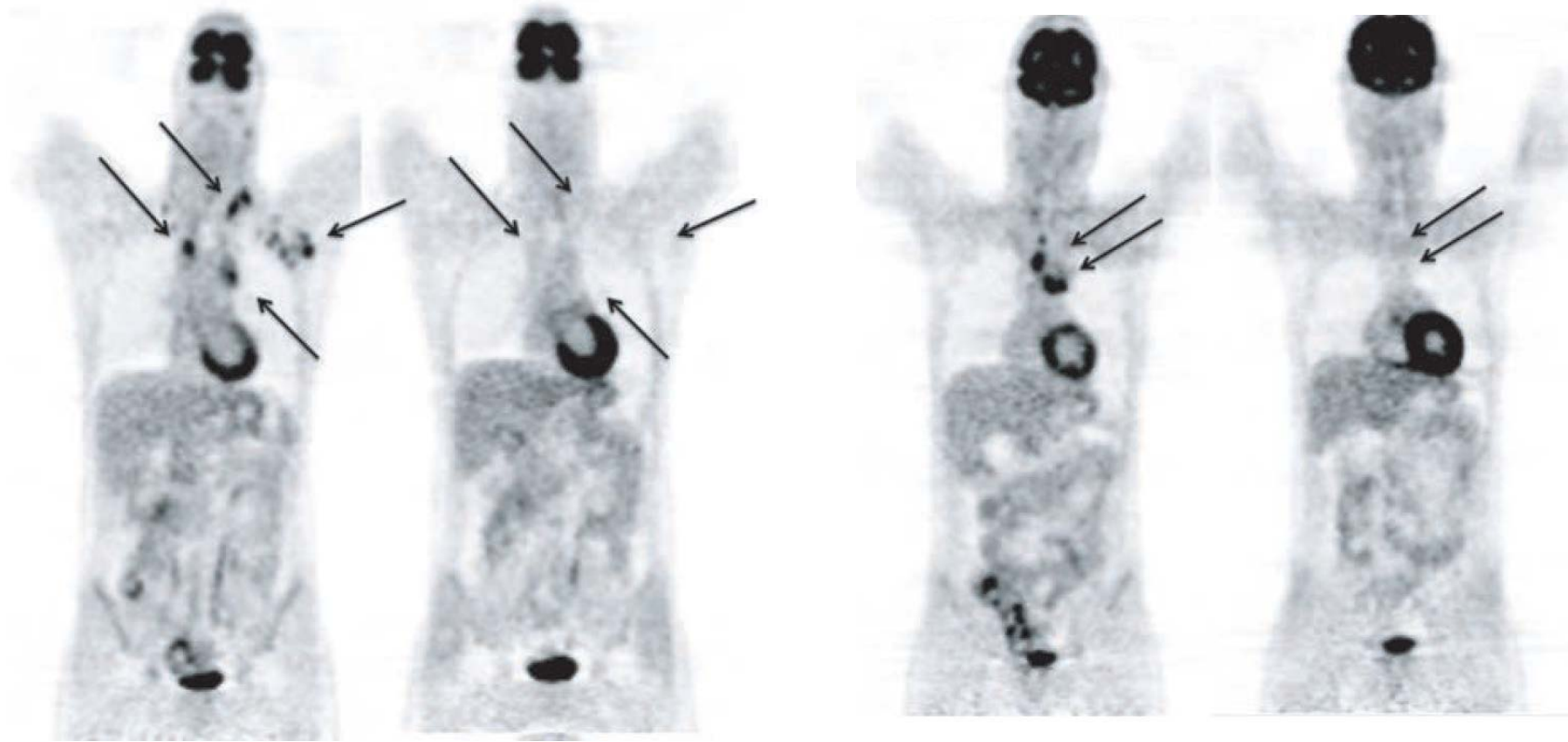


**Fig.**  $^{18}\text{F}$ FDG PET scan of a patient suffering from a lymphoma in the mediastinum and the left axilla (1 and 3). The pathological  $^{18}\text{F}$ FDG uptake in the lymphomatous lymph nodes (arrows) disappeared after chemotherapy (2 and 4)..

# Neurological disorders

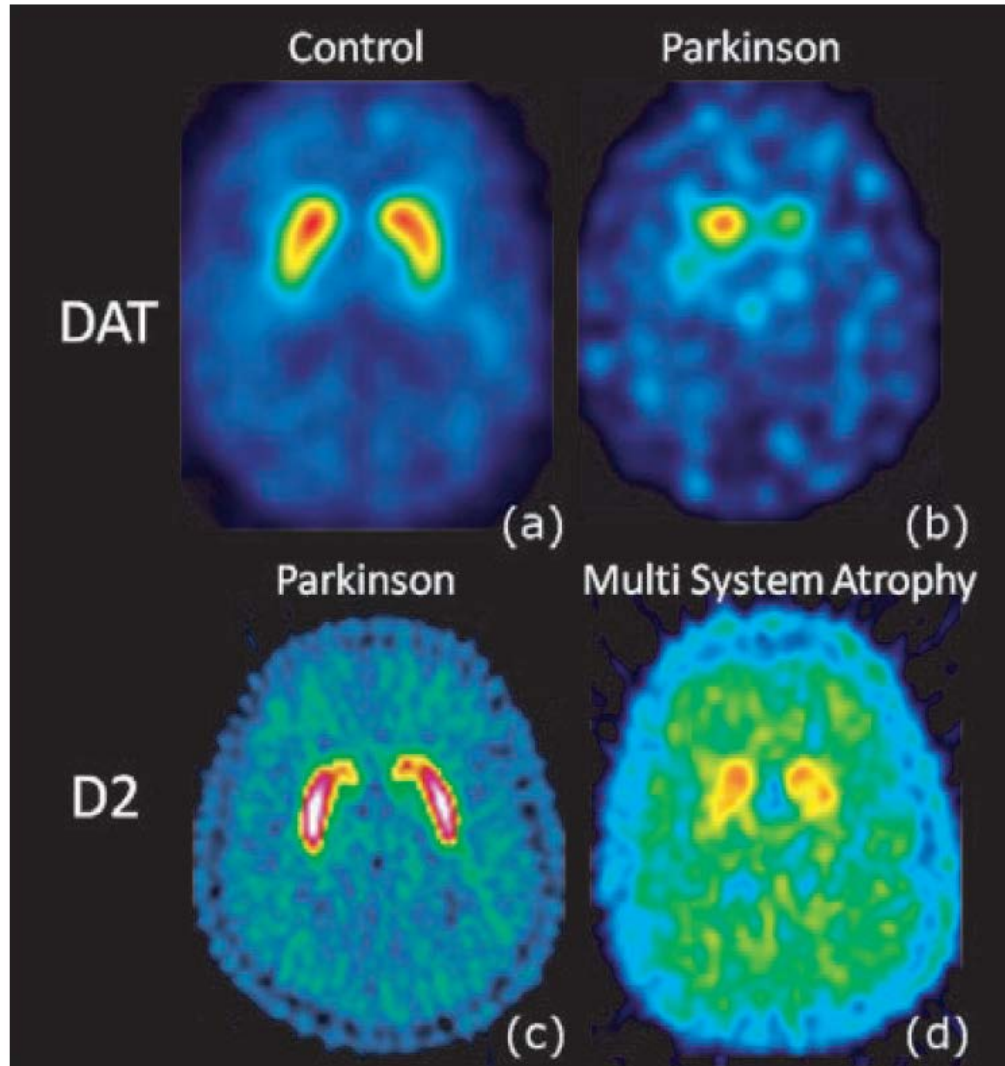


**Fig.** Upper row:  $^{123}\text{I}$ -FP-CIT SPECT scan for presynaptic dopamine transporter (DAT) imaging. Lower row:  $^{11}\text{C}$ -raclopride PET scan for postsynaptic dopamine receptor (D2) imaging. (a) Healthy subject. (b,c) In an early Parkinson patient a decrease of the dopamine transporter (DAT) is seen in the basal ganglia while the postsynaptic dopamine receptor (D2) is still normal. (d) Parkinson patient with multi-system atrophy (MSA). The postsynaptic part of the dopaminergic synapse is also impaired..